OVERHEATING INFLUENCE IN THE SOLIDIFICATION PARAMETERS AND MICROSTRUCTURE FORMATION OF ALUMINUM 5052 ALLOY

Rezende Gomes dos Santos
Department of Materials Science, Mechanical Engineering Faculty, C.P. 6122, State University of Campinas, CEP: 13.083 – 970, Campinas, SP, Brazil.
e-mail: rezende@fem.unicamp.br

Ricardo Batista de Andrade
Department of Materials Science, Mechanical Engineering Faculty, C.P. 6122, State University of Campinas, CEP: 13.083 – 970, Campinas, SP, Brazil.
e-mail: ricardo@fem.unicamp.br

Jean Robert Pereira Rodrigues
Department of Materials Science, Mechanical Engineering Faculty, C.P. 6122, State University of Campinas, CEP: 13.083 – 970, Campinas, SP, Brazil.
e-mail: jrobert@fem.unicamp.br

Tonnyfran Xavier de Araujo Sousa
Department of Materials Science, Mechanical Engineering Faculty, C.P. 6122, State University of Campinas, CEP: 13.083 – 970, Campinas, SP, Brazil.
e-mail: tonny@fem.unicamp.br

Mírian de Lourdes Noronha Motta Mello
PPG-ECM, São Francisco University (USF), Rua Alexandre de Rodrigues Barbosa Nº 45, CEP: 13.251 – 900, Itatiba, SP, Brazil.
e-mail: mirian.melo@saofrancisco.edu.br

Abstract. *The objective of this work is the development of a comparative analysis of solidification process of the aluminum 5052 alloy with different overheating ranges. The main parameters of the solidification process, experimentally determined, are affected by the overheating range and its influence on the microstructure arrangement. It was selected the 5052 alloy, containing about 3% of magnesium, used for commercial purposes. The alloy was poured with three different overheating ranges in a device which allows the unidirectional solidification and its monitoring through an acquisition data system thru the temperature variation from different positions on the sample. From the temperature results, the others process parameters are determined. The dendritic spacing is determined by the micrographs. Through experimental analysis is established the influence of the overheating range at the following parameters related to solidification process: heat transfer coefficient at the metal/mold interface, solidification rate, thermal gradient at the liquidus isotherm, cooling rate, local solidification time and secondary arm spacing. The change between the structure columnar and equiaxed is also studied.*

Keywords: *Unidirectional solidification, Al 5052 alloy, Overheating.*

1. Introduction:

Magnesium is the lightest of all metals used as the basis for constructional alloys. It is this property that entices automobile manufacturers to replace denser materials, not only steels, cast irons and copper base alloys but even aluminum alloys by magnesium-based alloys (Mordike and Ebert, 2001).

Numerical models for material properties prediction require validation to assure the developer and the user that the mechanics and numerical algorithms implemented in the model are correct and consistent with the experimental information available in the literature (Abbod *et al*, 2005).

The melted samples characteristics depend on thermal parameters of solidification, such as velocity at which the dendrite tip advances, thermal gradient at the liquidus isotherm, cooling rate and local solidification time, which directly affects the microstructure arrangement, thus the analysis of variation of these parameters in function of the solidification conditions is important.

It was selected the 5052 alloy, containing about 3% of Magnesium for commercial purposes. Alloys from Al-Mg group are ductile at the annealed state, but they harden quickly under cold work, have excellent weldability and high corrosion resistance on maritime environments. As applications they are used for: shutters, boats, signs, automobile bodies and stamping for general use (Alcan catalogue, 2005).

In this work a unidirectional solidification of 5052 alloy was realized, with three different overheating ranges; 720ºC, 750ºC e 780ºC and their relevance with the thermal parameters last mentioned and also their influence at the columnar zone size. Based on the facility of analysis, experiments that further the unidirectional solidification allow

to identify the interdendritic spacing as well as its relation with the solidification parameters and, so to do an analogy between others solidification methods. The primary dendritic arms, at the columnar structures, as well as the grain boundary, are aligned. The columnar structures' obtaining deserves emphasis also in the manufacturing of pieces that requires reliability, such as blades of jet engines. The blades manufactured with columnar structures present high resistance on longitudinal direction, because the grains are aligned at this same ultimate strain, which coincides with the centrifugal force direction. As the turbines work on high temperatures, the material must be resistant to the flow, which is promoted by the less number of grains boundary of columnar structure which decreases the significant action of the slip between them. In the case of the turbines, the alloys applied are nickel-basis (Garcia, 2001).

2. Experiments

The alloy used in this experimental work was the 5052 alloy containing about 3% of magnesium, which its composition is presented on table 1.

Table 1 – Chemical composition of Al-Mg alloy.

Al	Mg	Fé	Si	Cr	Mn	Cu	Others
95,510	3,091	0,593	0,383	0,242	0,142	0,038	0,001

The alloy was melted in an electric resistance furnace with three different overheating ranges, 720ºC, 750ºC and 780ºC respectively and then poured in an unidirectional solidification device, previously pre-heated near their respective fusion temperatures with the objective to avoid lateral loss of heat. Before the pouring, the furnace was turned off and then the cooling system is actuated.

The unidirectional solidification device, showed at Fig. 1, consists basically of a tubular furnace heated by four silicon carbide elements of globar type, which is fit into an insulating ceramic mold of zirconia measuring 280 mm length by 40 mm diameter that is coupled over a water cooled copper chill. This device was designed insomuch the heat abstraction could be accomplished only from the bottom cooled by water, furthering a vertical ascending unidirectional solidification. The variations of temperatures during the solidification process were measured by thermocouples, inserted at different positions on the sample, coupled to an acquisition data system of 12 bits of resolution compound of 2 conditioning boards, one board to 16 thermocouples type K e another to 16 thermocouples type S, with acquisition rate of 10 Hz by channel.

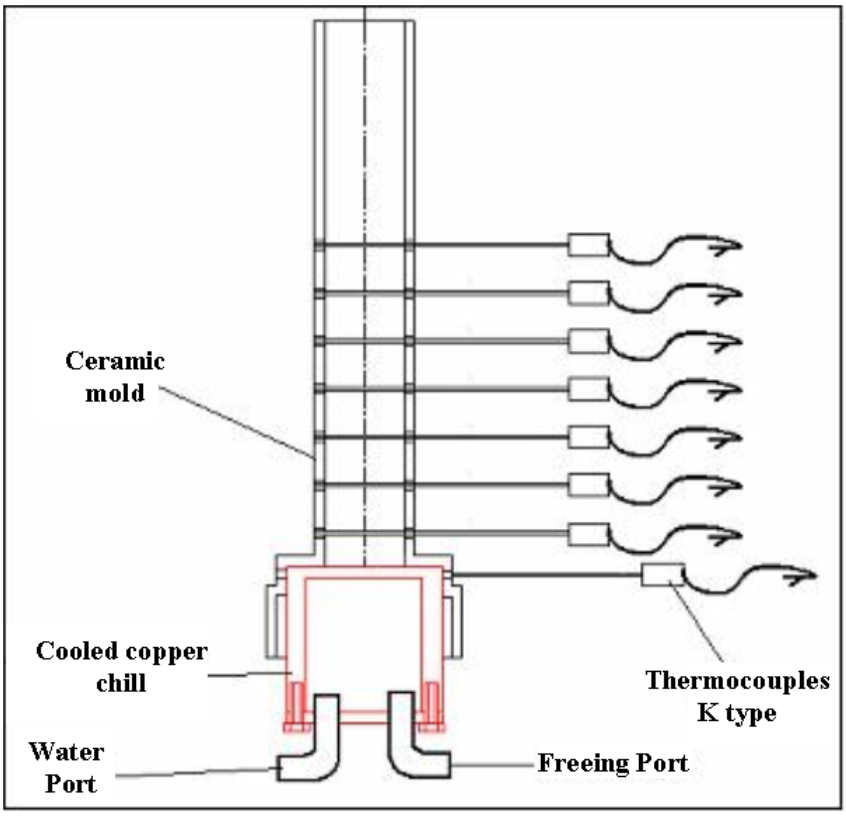

Figure 1 – Unidirectional solidification device.

Eight thermocouples type K were used (chromel-alumel), they were placed on the ceramic mold from the metal/mold interface and then connected to the acquisition data system. At the Fig. 2(a) is showed the copper chill and the ceramic mold and in the Fig. 2(b) a view of the furnace ready to be used.

(a) (b)

Figure 2 – (a) Copper chill and ceramic mold and (b) View of the furnace.

After, the sample is stripped and cut to lengthwise. One half was utilized for macrograph analysis and the other half for micrograph analysis. The samples obtained were polished and etched properly to reveal their macro and micrograph.

3. Results and discussion

Figures 3(a), (b) e (c) present as example, the results of temperatures acquiring to the different points inside the sample unidirectionally solidified of Al 5052 alloy to three different overheating ranges, 720ºC, 750ºC e 780ºC. The solidification time for the pouring temperature of 780ºC is high due to its elevated overheating range.

Figure 4 shows a variation of the heat transfer coefficient at the metal/chill interface determined through the comparing inverse method of experimental and numerical profiles to the Al 5052 alloy (Melo, 1996, 2005a, 2005b). From the comparatives results it is noticed that in the higher pouring temperature the efficiency of heat abstraction is elevated this happens owing to the higher overheating variation allowing a faster and intense heat exchanging. So, therefore it was obtained the most elevated heat transfer coefficient for the pouring temperature of 780ºC.

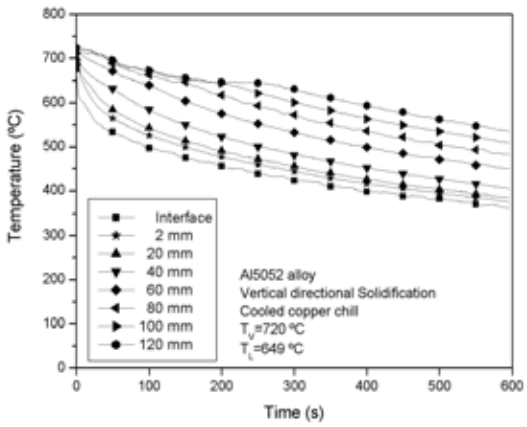

Figure 3(a) – Cooling curves to the Al 5052 alloy, 720º C.

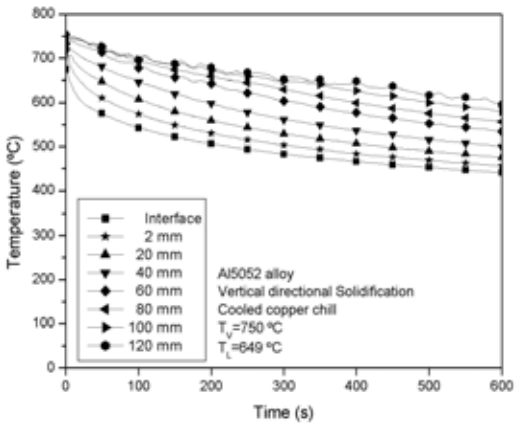

Figure 3(b) – Cooling curves to the Al 5052 alloy, 750º C.

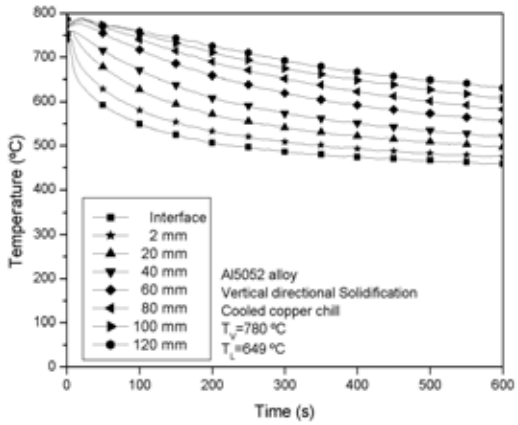

Figure 3(c) – Cooling curves to the Al 5052 alloy, 780º C.

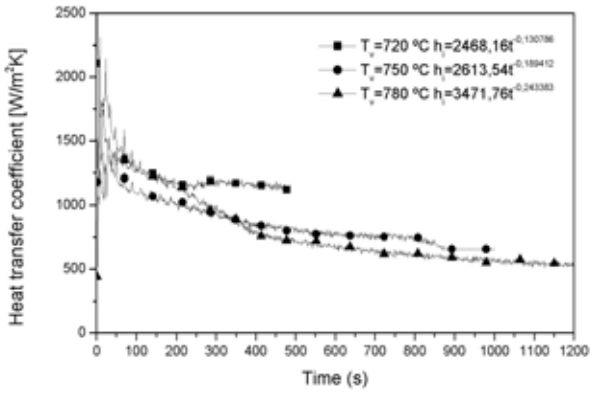

Figure 4 – Heat transfer coefficient.

The macrographs results of the performed experiments present a large extension of columnar grains, as result of the unidirectional solidification, indicating the efficiency of the developed device.

Figures 5(a), (b) e (c) show the macrographs obtained from the Al 5052 alloy poured in 720ºC, 750ºC e 780ºC respectively. It is possible to see a progressive increasing of the columnar zone as long as the pouring temperatures increase. The extension of each columnar zone is: to 720º C-85mm, 750º C-110mm and 780º C-125mm. It is possible to visualize columnar grains until to the maximum length of 125mm in the pouring temperature of 780º C. The samples were etched by rubbing using the following etchant for revealing their macrostructures: 20 mL glycerin, 30 mL HCl, 2 mL satured aqueous, $FeCl_3$ solution, 7 drops HF and 1 mL of HNO_3.

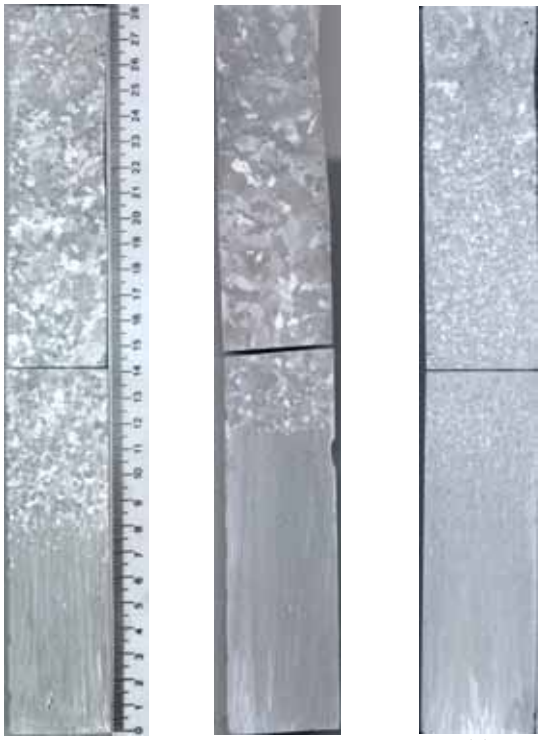

(a) (b) (c)

Figure 5 – Macrographs of Al 5052 alloy pouring at: (a) 720ºC, (b) 750ºC and (c) 780ºC.

The temperatures and the time acquired on the files from the acquisition data system were utilized to the determination of the experimental thermal parameters.

The position of liquidus isotherm in function of the time it is a parameter that could be directly determined from the cooling curves, which is showed at Fig. 6. The solidification time it is high for the alloy poured at 780ºC due to its higher overheating range. As the pouring temperature of 720ºC is near of liquidus line it is possible to perceive the solidification time is the lesser.

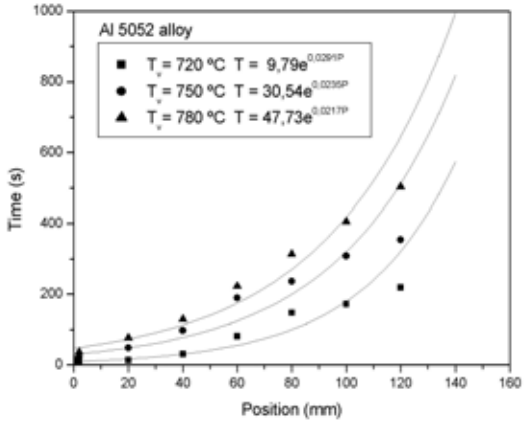

Figure 6 – Variation curves of liquidus isotherm positions in function of time to the three different overheating ranges.

Figure 7 presents a variation of the velocity at which the dendrite tip advances in function of the position to the three overheating ranges. This parameter is obtained from the cooling curves corresponding to each thermocouple, accepting the temperature on the dendrite tip be the same as liquidus temperature (Pan and Loper Jr., 1990; Suri *et al.*, 1994; Laurent and Rigaut, 1992; Melo *et al.*, 2004):

At Fig. 7 it is observed a decreasing on the velocities at which the dendrite tip advances on the positions further from the cooled chill, this is owing to the increasing of the solidified layer with the progress of the solidification process, applying a resistance to the heat flow. So, it is set a time (*t'*) where the liquidus isotherm pass through the position corresponding to a determinate thermocouple and the time (*t''*) that it crossed the position corresponding to the next thermocouple. The two thermocouples distance (Δx) is divided by the time interval, so it is acquired the velocity at which the dendrite tip advances (v):

$$v = \frac{\Delta r}{t'' - t'} \tag{1}$$

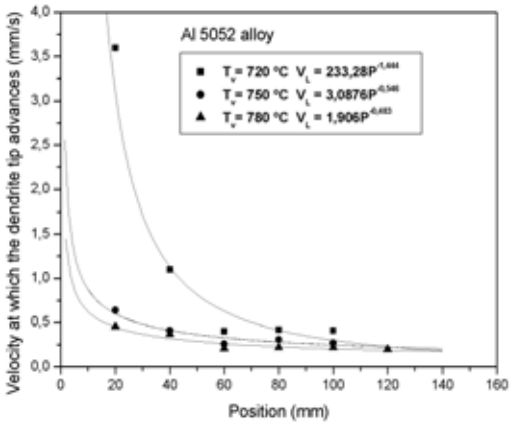

Figure 7 – Variation curves of velocities at which the dendrite tip advances in function of position to the different overheating ranges.

Figure 8 presents the variations of thermal gradient at the liquidus isotherm for the three different overheating ranges. This figure shows a decreasing of the temperature gradients for the overheating ranges as the solidification advances, due to the gradual dissipation of liquid metal overheated.

The thermal gradient at the liquidus isotherm (G) is acquired by the difference between T_{liq}, which is the liquidus temperature corresponding to the position of determinate thermocouple, and *T'* that is the temperature corresponding to the position of next thermocouple divided by Δx, which is the distance between them, as it is seeing below:

$$G = \frac{T' - T_{liq}}{\Delta x} \tag{2}$$

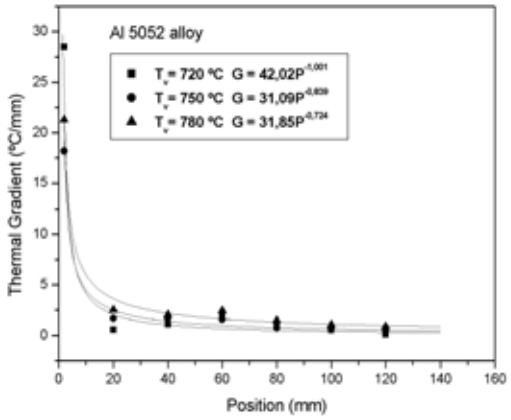

Figure 8 – Thermal gradient in function of the position.

Thru the velocities at which the dendrite tip advances (v) and the thermal gradients (G) were determined the cooling rates during the solidification through the following relation:

$$\dot{T} = G \cdot v \tag{3}$$

Analyzing comparatively the variation curves of the cooling rates for the alloy studied as showed at Fig. 9, it is noticed that the rates are higher for the Al 5052 alloy poured at 720ºC owing to the higher cooling velocity. As the solidification advances the rates to the others overheating ranges lean to proximate values due to the overheating dissipation and consequent thermal gradient decreasing.

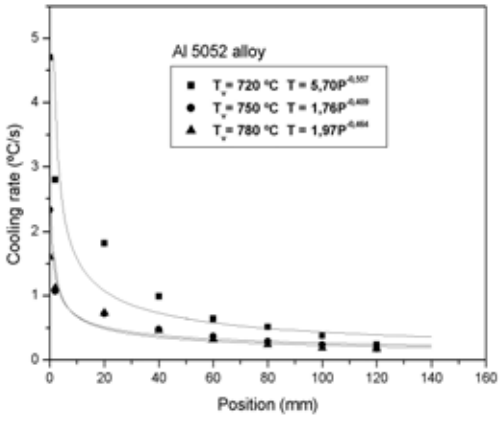

Figure 9 – Cooling rates.

The micrographs were obtained on the longitudinal section from the three pouring temperature in the middle of their regions at the columnar zone as it is showed in the Fig. 10(a), (b), (c). The samples were sequencing etched by immersion using the same etchant for the macrograph. It is observed that the appearing of dendrites is more evident from the intermediate zone to the end of columnar zone and also with the temperature overheating increasing.

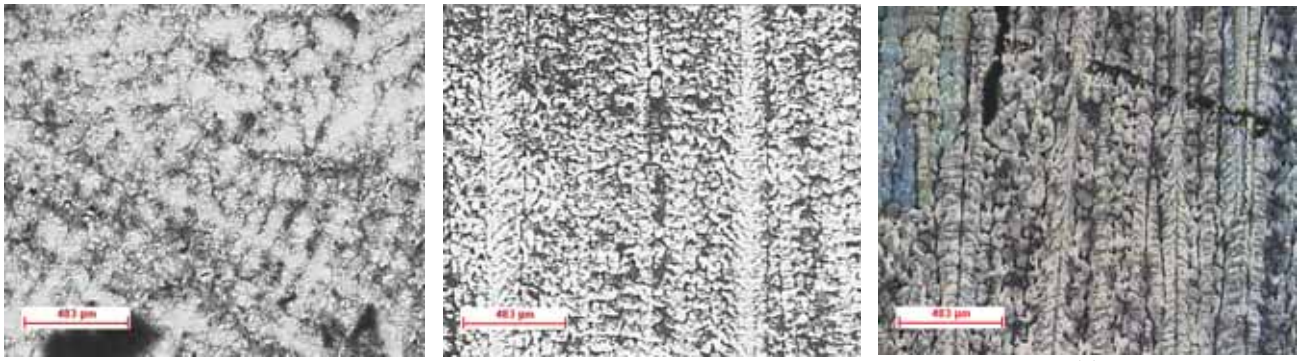

(a) (b) (c)

Figure 10 – Micrograph at the longitudinal section in the middle of the columnar zone to each pouring temperature: 720ºC (a), 750ºC (b) and 780ºC (c).

The secondary dendrite arms spacing were experimentally measured along the columnar zone in function of the position for the three pouring temperature as presented at the Fig. 11. In the pouring temperatures of 720ºC and 750ºC it was more difficult to measure the dendritic secondary arms spacing in the beginning of columnar zone owing to their elevated refinement degree. Nevertheless it was possible to observe the increasing of their size as they are further from the metal/chill interface (Santos and Melo, 2005).

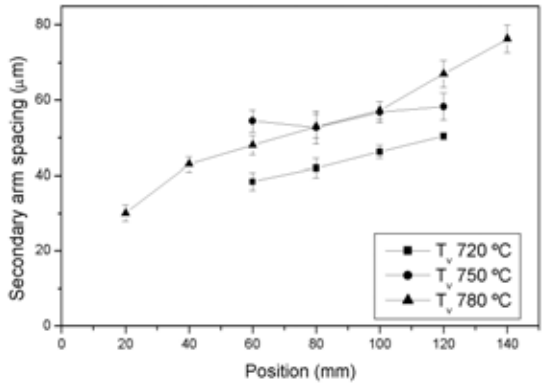

Figure 11 – Secondary arm spacing

4. Conclusions

The acquired results in this work allow concluding that the unidirectional solidification device built it is efficient and admits the obtainment of extended columnar zones of 85 mm, 110 mm and 125 mm to the respectively pouring temperatures of 720ºC, 750ºC and 780ºC.

The solidification time for the pouring temperature of 780ºC is high due to its most elevated overheating range.

From the comparatives results it is noticed that in the higher pouring temperature the efficiency of heat abstraction is elevated this happens owing to the higher overheating variation allowing a faster and intense heat exchanging. So, therefore it was obtained the most elevated heat transfer coefficient for the pouring temperature of 780ºC.

It is possible notice the velocities at which the dendrite tip advances decrease on the positions more distant from the cooled chill owing to the progressive increasing of the solidified layer with the solidification process evolution, imposing a higher resistance to the heat flow.

The thermal gradient for the overheating ranges decreases as the solidification advances owing to the gradual dissipation of the overheated liquid metal. Because of its proximity with the liquidus line the thermal gradient presents the lowest value to the pouring temperature of 720ºC.

Analyzing comparatively the variation curves of the cooling rates for the alloy studied, it is noticed that the rates are higher for the Al 5052 alloy poured at 720ºC owing to the higher cooling velocity. As the solidification advances the rates to the others overheating ranges lean to proximate values due to the overheating dissipation and consequent thermal gradient decreasing.

The micrographs corresponding to the beginning of columnar zone reveal an elevated degree of refinement, so it was only possible measure the dendrite secondary arms spacing at the regions further from the interface.

5. Acknowledgements

The authors thank to FAPESP, FAPEMA, CAPES and CNPq by their financial support on the development of this work.

6. References

Abbod, M.F., Sellars, C.M., Linkens, D.A., Zhu, Q., Mahfouf, M., 2005, "Validation and generalization of hybrid models for flow stress and recrystallisation behavior of aluminium–magnesium alloys", Materials Science and Engineering A, Vol.395, pp. 35-46.

Aluminum Canada, 2005, Alcan catalogue, http://www.alcan.com.

Garcia, A., 2001, "Solidificação:Fundamentos e Aplicações", Ed. da Unicamp, Campinas, SP, Brazil, 399 p.

Laurent, V., Rigaut, C., 1992, "Experimental an Numerical Study of Criteria Functions for Predicting Microporosity in Cast Aluminium Alloys", AFS Transactions, Vol.100, pp. 647-655.

Melo, M. L. N. M., 1996, "Análise Numérico/Experimental da Formação de Microporosidades Durante a Solidificação de Ligas de Alumínio", Tese (Doutorado) - Faculdade de Engenharia Mecânica, Unicamp, Campinas, 254 p.

Melo, M. L. N. M., Rizzo; E. M. S. and Santos, R. G., 2004, "Numerical model to predict the position, amount and size of microporosity formation in Al-Cu alloys by dissolved gas and solidification shrinkage", Materials Science and Engineering A, Vol.374, pp. 351-361.

Melo, M. L. N. M., Rizzo, E. M. S. and Santos, R. G., 2005, "Prediction of dendrite Arm spacing and its effect on microporosity formation in directionally solidified Al-Cu Alloy", Journal of Materials Science, Vol.40, pp. 1-11.

Melo, M. L. N. M., Santos, C.A., Penhalber, C.A.L., 2005, "Determinação numérico/experimental do coeficiente de transferência de calor na interface metal/molde durante a solidificação do aço inoxidável AISI 304", Revista Matéria, Accepted for publishing.

Mordike, B.L., Ebert, T., 2001, "Magnesium, Properties-applications-potential", Materials Science and Engineering A, Vol.302, pp. 37-45.

Pan, E.N., LIN, C.S., Loper, Jr, C.R., 1990, "Effects of Solidification Parameters on the Feeding Efficiency of A356 Aluminum Alloy", AFS Transactions, Vol.98, pp. 735-746.

Suri, V. K., Paul, A. J., Berry, J. T., 1994, "Determination of Correlation Factors for Prediction of Shrinkage in Castings – Part I: Prediction of Microporosity in Casting; a Generalized Criterion", AFS Transactions, Vol.102, pp. 861-867.

Santos, R. G.; Melo, M. L. N. M., 2005, "Permeability of interdendritic channels", Materials Science and Engineering A-Structural Materials Properties Microstructure and Processing, England, Vol.391, pp. 151-158.